

# Dalton Transactions

Accepted Manuscript



This is an *Accepted Manuscript*, which has been through the Royal Society of Chemistry peer review process and has been accepted for publication.

*Accepted Manuscripts* are published online shortly after acceptance, before technical editing, formatting and proof reading. Using this free service, authors can make their results available to the community, in citable form, before we publish the edited article. We will replace this *Accepted Manuscript* with the edited and formatted *Advance Article* as soon as it is available.

You can find more information about *Accepted Manuscripts* in the [Information for Authors](#).

Please note that technical editing may introduce minor changes to the text and/or graphics, which may alter content. The journal's standard [Terms & Conditions](#) and the [Ethical guidelines](#) still apply. In no event shall the Royal Society of Chemistry be held responsible for any errors or omissions in this *Accepted Manuscript* or any consequences arising from the use of any information it contains.

**Phenolate Based Metallomacrocyclic Xanthate Complexes of Co<sup>II</sup>/ Cu<sup>II</sup> and Their Exclusive Deployment in [2:2] Binuclear *N, O*-Schiff Base Macrocycle Formation and *in vitro* Anticancer Studies<sup>†</sup>**

Vinay K. Singh,<sup>\*a</sup> Rahul Kadu,<sup>a</sup> Hetal Roy,<sup>b</sup> Pallegogu Raghavaiah<sup>c</sup> and Shaikh M. Mobin<sup>d</sup>

<sup>†</sup> Dedicated to Professor Pradeep Mathur on the occasion of his 60<sup>th</sup> Birthday

<sup>a</sup>Department of Chemistry, Faculty of Science, The M. S. University of Baroda, Vadodara-390 002, India

<sup>b</sup>Department of Zoology, Faculty of Science, The M. S. University of Baroda, Vadodara-390 002, India

<sup>c</sup>Department of Chemistry, Dr. Harisingh Gour University, Sagar-470003, India

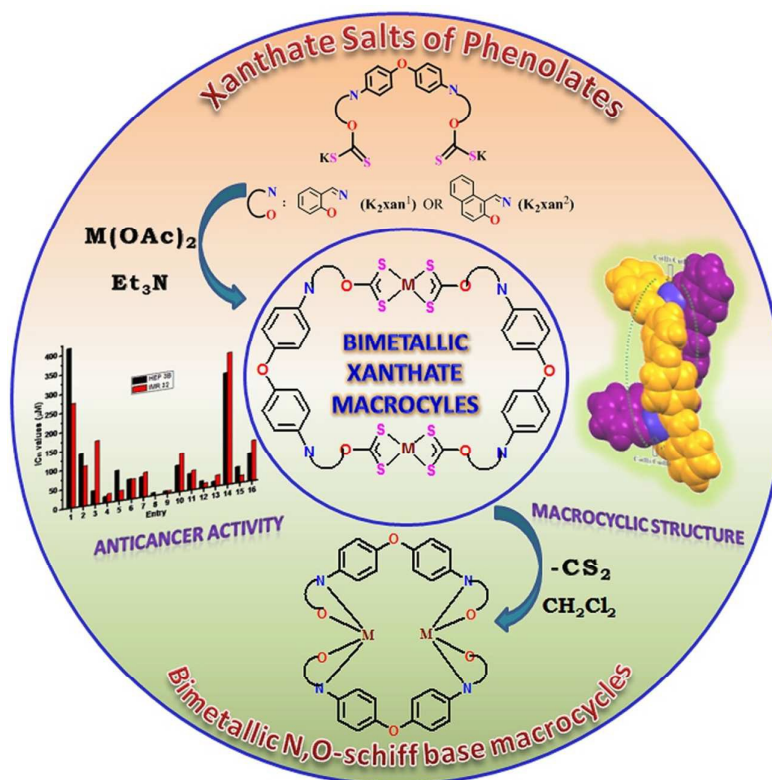
<sup>d</sup>Department of Chemistry, Indian Institute of Technology Indore-452 017, India

\*Email: [vinay.singh-chem@msu.ac.in](mailto:vinay.singh-chem@msu.ac.in)

**Table of contents entry**

Crystallographic and *in vitro* anticancer studies of phenolate based Co<sup>II</sup>/ Cu<sup>II</sup> xanthate metallomacrocycles and their *N, O*-Schiff base derivatives.

**Graphics:**



**Abstract:** Potassium salts of phenolate based polydentate xanthate ligands 4,4'-bis(2-dithiocarbonatobenzylideneamino)diphenyl ether ( $K_2xan^1$ ) and 4,4'-bis(2-

dithiocarbonatonaphthylmethylideneamino)diphenyl ether ( $\mathbf{K}_2\mathbf{xan}^2$ ) have been synthesized and characterized, prior to use. Reaction of  $\mathbf{K}_2\mathbf{xan}^1$  or  $\mathbf{K}_2\mathbf{xan}^2$  with  $\text{M}(\text{OAc})_2$  in  $\text{Et}_3\text{N}$  affords access to a rare series of binuclear metallomacrocyclic xanthate complexes of the type  $[\text{M}_2-\mu^2\text{-bis}-(\kappa^2\text{S},\text{S-xan}^1/\text{xan}^2)]$  (**1-4**) which quickly forms [2:2] binuclear *N, O*- bidentate Schiff base macrocyclic complexes of the type  $[\text{M}_2-\mu^2\text{-bis}-(\kappa^2\text{N},\text{O-L}^1/\text{L}^2)]$  ( $\mathbf{L}^1 = 4,4'$ -bis(2-hydroxybenzylideneamino)diphenyl ether,  $\mathbf{L}^2 = 4,4'$ -bis(2-hydroxynaphthylmethylideneamino)diphenyl ether) **5-8** *via* evolution of  $\text{CS}_2$  in solution. Compounds were characterized by microanalysis, relevant spectroscopy (FT-IR, UV-visible), mass spectrometry (ESI-MS), powder and single crystal XRD techniques. *In vitro* anticancer activity of all the compounds was evaluated against HEP 3B (Hepatoma) and IMR 32 (Neuroblastoma) by the MTT assay. Remarkably, the binuclear copper(II) xanthate complexes were found extremely active against both the cell lines ( $\text{IC}_{50}$ :  $8.1 \pm 0.8 \mu\text{M}$  (**3**),  $8.8 \pm 1.7 \mu\text{M}$  (**4**) against HEP 3B and  $1.9 \pm 0.3 \mu\text{M}$  (**3**) and  $7.3 \pm 0.6 \mu\text{M}$  (**4**) against IMR 32) and this projects them in the vein of good candidates as potent antitumor agent and the  $\text{IC}_{50}$  values confirm their better potency than the reference drug cisplatin. Flow-cytometric density plot illustrates the induction of apoptosis in HEP 3B and IMR 32 cells after the treatment with  $\mathbf{K}_2\mathbf{xan}^1$ , **1**, **3**, **6** and **7**.

**Keywords:** Xanthate, Schiff base, metallomacrocyclic, XRD, anticancer activity.

---

## Introduction

The interest in the chemistry of discrete metallomacrocyclic structures with diverse cavity size and shape<sup>1</sup> has been continued due to their potential applications in catalysis,<sup>2</sup> host-guest chemistry,<sup>3</sup> molecular and ion sensing,<sup>4</sup> separation, transport and storage,<sup>5</sup> in drug delivery, two-phase transport and biosensing.<sup>6</sup> In particular, transition metal complexes offer additional opportunities for development of new therapeutic agents not accessible to organic

compounds,<sup>7</sup> by means of varied coordination numbers, geometries, redox states, thermodynamic-kinetic characteristics, and intrinsic properties of both metal ions and ligands. The platinum based anticancer drug, cisplatin and its analogues have already proved to be indispensable in cancer chemotherapy. The efforts in the evaluation of anticancer drugs have been shifted to non-platinum metal-based agents that have improved pharmacological properties and aimed at different targets,<sup>8</sup> to avoid dose-limiting side effects<sup>9</sup> and due to the emergence of drug resistance associated with platinum chemotherapeutics.<sup>10</sup> In this context, copper and cobalt complexes have shown encouraging results,<sup>11, 12</sup> mainly due to their redox activity and accessibility for transmetallation.

A careful literature search revealed that a wide range of natural product bearing macrocyclic motif and their synthetic derivatives have long been clinically used as they offer structural pre-organization with sufficient flexibility for better binding with the target molecules and exhibit high degree of potency as well as selectivity.<sup>13</sup> However, a class of inorganic compounds “metallomacrocyclic structures” have scarcely been investigated<sup>14,15</sup> from a medical perspective especially for antitumor activity. Very recently, we have developed a series of binuclear diphenyltin<sup>IV</sup>dithiocabamate macrocyclic scaffolds  $[(\text{Ph}_2\text{Sn}^{\text{IV}})_2-\mu^2\text{-bis-}\{(\kappa^2\text{S,S-S}_2\text{CN}(\text{R})\text{CH}_2\text{CONHC}_6\text{H}_4)_2\text{O}\}]$  {R = *i*Pr (1), *s*Bu (2), *n*Bu (3), Cy (4), 2-furfuryl (5) or benzyl (6) that have shown exceptional anticancer activity against Neuroblastoma and Hepatoma human cancer cell lines.<sup>15</sup> Sulfur being an important constituent of biomolecules, plays a crucial role in transporting and addressing the molecule to the targets as well as in the protection of the pharmacophore against untimely exchanges with biomolecules.<sup>9,16</sup> Sulfur-rich compounds exhibit good DNA/protein binding/cleaving and catalytic activity toward glutathione.<sup>17</sup> Besides, Schiff bases have also been used in the preparation of many potential drugs that are known to possess a broad spectrum of biological activities.<sup>18</sup> Literature suggests that when administered as their metal complexes, the

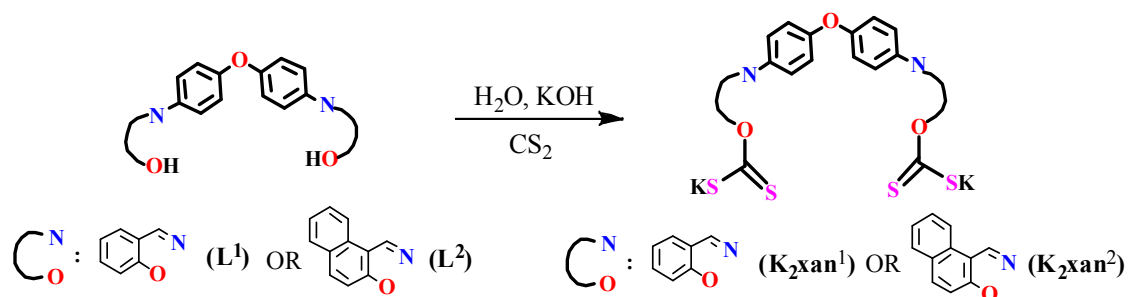
anticancer activity of these complexes is enhanced in comparison to the free Schiff base ligands.<sup>19</sup> Moreover, metal complexes derived from salicylaldehyde is known to cleave DNA.<sup>20</sup>

Tanaka et al.,<sup>21</sup> have reported primary investigations on *in-vivo* mutagenicity of 4,4'-diaminodiphenyl ether and its *N*-acetyl derivative towards *Salmonella typhimurium* TA98 and TA100 in 1985. However there are very few reports<sup>15,22</sup> on further investigations of biological properties of 4,4'-diaminodiphenyl ether and its derivatives. In this contribution, we have synthesized potassium salts of 4,4'-bis(2-dithiocarbonatobenzylideneamino)diphenyl ether (**K<sub>2</sub>xan<sup>1</sup>**) and 4,4'-bis(2-dithiocarbonatonaphthylmethylideneamino)diphenyl ether (**K<sub>2</sub>xan<sup>2</sup>**). Phenolate based xanthate **K<sub>2</sub>xan<sup>1</sup>** and **K<sub>2</sub>xan<sup>2</sup>** ligands have been used to derive binuclear metallomacrocyclic Co<sup>II</sup>/ Cu<sup>II</sup> xanthate complexes **1-4**. Interestingly **1-4** undergo a facile transformation into their corresponding (2:2) binuclear metallomacrocyclic *N,O*-Schiff base complexes **5-8**, selectively. In a conventional approach for the synthesis of (2:2) binuclear metallomacrocyclic *N,O*-Schiff base complexes, lack of selectivity appears to be the main barrier. To the best of our knowledge, this is the first report on binuclear metallomacrocyclic xanthate complexes derived from phenolate based polydentate xanthate ligands and their selective transformations into (2:2) binuclear *N,O*-Schiff base macrocycles. All the compounds were investigated for their potential *in vitro* cytotoxic and apoptosis inducing properties against HEP 3B and IMR 32 human cancer cells. With anticipation, the incorporation of the xanthate moiety in the molecular framework of the ensuing complexes would enhance the possibility of stacking and intercalation through a number of noncovalent interactions with DNA/proteins and may lead to the superior anticancer activity.

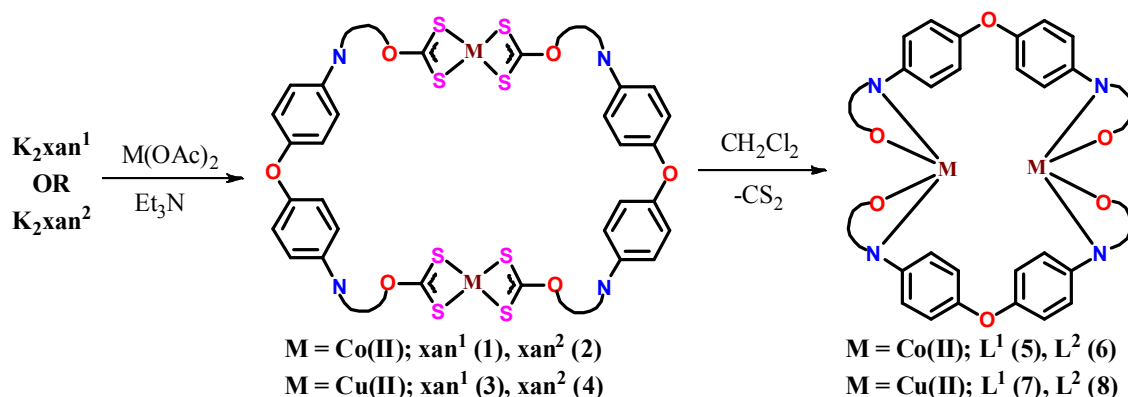
## Results and discussion

### Synthesis and characterization

Ligand precursors 4,4'-bis(2-hydroxybenzylideneamino) ether ( $L^1$ ) and 4,4'-bis(2-hydroxynaphthylmethylideneamino)diphenyl ether ( $L^2$ ) have been synthesized by using a literature procedure<sup>23</sup> (Scheme S1). The potassium salts of polydentate xanthate ligands ( $K_2xan^1$  or  $K_2xan^2$ ) were synthesized by the reaction of these phenolates  $L^1$  or  $L^2$  with  $CS_2$  in the aqueous KOH solution shown in Scheme 1. Though numerous reports support the easy accessibility of xanthate ligands derived from alcohols and their use in synthetic organic,<sup>24</sup> coordination<sup>25</sup> chemistry, the use of phenolates based xanthates in the development of metallomacrocyclic coordination compounds have not yet been investigated. The lack of stability of transition metal xanthate complexes,<sup>31</sup> primarily limit their use in coordination chemistry. However, we could use phenolate based  $K_2xan^1$  and  $K_2xan^2$  ligands successfully to derive binuclear metallomacrocyclic  $Co^{II}/Cu^{II}$  xanthate complexes **1-4** (Scheme 2) from a metathetical reaction of  $K_2xan^1$  or  $K_2xan^2$  with corresponding metal acetates in  $Et_3N$ .



**Scheme 1.** General scheme for the synthesis of  $K_2xan^1$  and  $K_2xan^2$ .



**Scheme 2.** General synthetic methodology used for binuclear  $Co^{II}/Cu^{II}$  xanthate metallomacrocycles and their respective binuclear  $N,O$ -bidentate Schiff-base analogues.

These complexes **1-4** are stable in the solid state but are found to be unstable, especially in chlorinated solvents. The instability associated with the binuclear metallomacrocyclic Co<sup>II</sup>/ Cu<sup>II</sup> xanthate complexes **1-4** helped us to use them further in selective transformation reactions leading to the corresponding (2:2) binuclear metallomacrocyclic *N,O*-Schiff base complexes **5-8**.

Literature suggests that a direct approach to obtain (2:2) binuclear Schiff base metallamacrocycles suffer the disadvantage of giving a mixture of products *viz.* 1:1, 2:2, 3:3, 4:4 and the (1:1)<sub>∞</sub> polymeric species which are insoluble in most organic solvents.<sup>27</sup> Further reports suggest that the conformational modes of the ligand, nuclearity and ultimately the structures of the resulting complexes, greatly depend upon the selection of metal ion. For instance, J. Zhang *et. al.* have isolated a dinuclear mesocate structure for Cu<sup>II</sup> and a pseudo C<sub>3</sub>-symmetrical torus-like molecular structure for Co<sup>II</sup> ions with the same ligand system.<sup>28</sup> Hence, in the development of efficient synthetic methodology for the formation of binuclear metallomacrocyclic complexes, lack of selectivity is one of the main barriers. Thus, the present synthetic methodology to obtain (2:2) binuclear metallomacrocyclic *N, O*-Schiff base complexes selectively from their respective binuclear metallamacrocyclic Co<sup>II</sup>/Cu<sup>II</sup> xanthate complexes is of great interest. The presence of Schiff base (-N=C) moiety in close proximity to xanthate (-OCS<sub>2</sub>) moiety in **1-4**, causes instability in solution, enforcing these molecules to undergo a facile transformation into their corresponding (2:2) binuclear metallomacrocyclic *N, O*-Schiff base complexes **5-8** selectively, *via* CS<sub>2</sub> evolution which was easily detected by GC. Earlier, CS<sub>2</sub> evolution from 1,1-dithiolato complexes in chlorinated solvents has been observed.<sup>29</sup> Moreover, the isolation of binuclear metallamacrocyclic Co<sup>II</sup> xanthate complexes became possible due to the poor electron density at Co<sup>II</sup> centers, apparently revealed by DFT study (Table S13), thereby preventing them from ready oxidation, unlike earlier reports.<sup>30</sup>

The newly synthesized compounds were characterized by elemental, ES-MS, thermogravimetric analysis and relevant spectroscopic techniques. The microanalysis and spectroscopic data were sufficient to unequivocally assign the structure of potassium salts of xanthate ligands  $\mathbf{K}_2\mathbf{xan}^1$  and  $\mathbf{K}_2\mathbf{xan}^2$ . The IR spectra of these ligands display characteristic IR bands due to  $\nu(\text{C}=\text{N})$ ,  $\nu(\text{C}-\text{O})$  and  $\nu(\text{CS}_2)$  in the region of 1619-1624, 1084-1147 and 982-1038  $\text{cm}^{-1}$  respectively. In the  $^1\text{H}$  NMR spectrum, the disappearance of phenolic -OH signals and significant downfield shift of imine ( $-\text{N}=\text{CH}$ ) signals to the 8.97 and 9.688 ppm are indicative of the formation of  $\mathbf{K}_2\mathbf{xan}^1$  and  $\mathbf{K}_2\mathbf{xan}^2$ , respectively. In the  $^{13}\text{C}$  NMR spectra, most characteristic signals appeared at 190.86 and 190.24 ppm due to the xanthate ( $-\text{OCS}_2$ ) moiety, apart from the signals that appeared in the regions 161.83-168.69 ppm and 108-162 ppm due to the imine ( $-\text{N}=\text{CH}$ ) and aromatic groups respectively. The IR spectra of binuclear xanthate complexes **1-4** exhibit most characteristic bands in the region 1041-967  $\text{cm}^{-1}$ , diagnostic of *S,S* coordination of the xanthate ligands.<sup>31</sup> The appearance of shoulder or split bands in the region of 1041-967  $\text{cm}^{-1}$ , is indicative of anisobidentate coordination mode of the xanthate moiety in **1-4**. The absence of  $-\text{OCS}_2$  bands and subsequent splitting of  $\nu(\text{C}=\text{N})$  stretching bands with significant shifting (compared to  $\nu(\text{C}=\text{N})$  bands in  $\mathbf{L}^1$  or  $\mathbf{L}^2$ ) in the IR spectra of **5-8** suggests the formation of corresponding binuclear metallomacrocyclic *N,O*-Schiff base complexes. The structural variations in  $\mathbf{K}_2\mathbf{xan}^1$ , its binuclear xanthate complex **1** and the corresponding binuclear *N,O*-Schiff base complex **5** can easily be seen in their overlapped IR spectra. (Supporting Information)

**Table 1** UV-visible and fluorescence bands for  $\mathbf{L}^1$ ,  $\mathbf{L}^2$ ,  $\mathbf{K}_2\mathbf{xan}^1$ ,  $\mathbf{K}_2\mathbf{xan}^2$  and **1-8**.

| Entry                        | UV-Visible data ( $10^{-4}$ M DMSO)  | Fluorescence data ( $10^{-4}$ M DMSO) |                            |
|------------------------------|--|---------------------------------------|----------------------------|
|                              | $\lambda_{\text{max}}$ nm ( $\epsilon$ , $\text{L mol}^{-1} \text{cm}^{-1}$ )            | $\lambda_{\text{em}}$ nm (Intensity)  | $\lambda_{\text{ex}}$ (nm) |
| $\mathbf{L}^1$               | 320 (15633) $\pi \rightarrow \pi^*$ , 364 (13555) $n \rightarrow \pi^*$ , 395 CT         | 432 (16.0497), 513 (6.1781)           | 360                        |
| $\mathbf{L}^2$               | 319 (26530) $\pi \rightarrow \pi^*$ , 365 (21589) $n \rightarrow \pi^*$ , 480 (17534) CT | 519 (25.7266)                         | 318                        |
| $\mathbf{K}_2\mathbf{xan}^1$ | 319 (26530) $\pi \rightarrow \pi^*$ , 367 (21589) $n \rightarrow \pi^*$ , 444 (7920) CT  | 520 (9.5477)                          | 366                        |
| $\mathbf{K}_2\mathbf{xan}^2$ | 321 (28560) $\pi \rightarrow \pi^*$ , 366 (24090) $n \rightarrow \pi^*$ , 490 (19778) CT | 532 (57.9323)                         | 497                        |

|   |   |                                |          |
|---|---|--------------------------------|----------|
| 1 | 318 (32593) $\pi \rightarrow \pi^*$ , 366 (27634) $n \rightarrow \pi^*$ ,<br>405 (15852) CT, 531 d-d                                    | 469 (11.1489),<br>519(12.6580) | 364      |
| 2 | 316 (53760) $\pi \rightarrow \pi^*$ , 367 (39718) $n \rightarrow \pi^*$ ,<br>433 (34477) CT, 556 d-d                                    | 634 (21.6423)                  | 317      |
| 3 | 314 (4903) $\pi \rightarrow \pi^*$ , 348 (4032) $n \rightarrow \pi^*$ ,<br>380 (4534) $n \rightarrow \pi^*$ , 452 (4156) CT,<br>683 d-d | 628(32.09)                     | 314      |
| 4 | 317 (6527) $\pi \rightarrow \pi^*$ , 366 (5346) $n \rightarrow \pi^*$ ,<br>461(4959) CT, 674 d-d  | 634 (14.013)                   | 317      |
| 5 | 314 (35817) $\pi \rightarrow \pi^*$ , 349 (29221) $n \rightarrow \pi^*$ ,<br>390 CT, 538 d-d  | 410 (178.54)                   | 314      |
| 6 | 317 (36314) $\pi \rightarrow \pi^*$ , 365 (30300) $n \rightarrow \pi^*$ ,<br>458 (28921) CT, 565 d-d                                    | 545 (21.5474)<br>634 (40.7225) | 317      |
| 7 | 318 (5726) $\pi \rightarrow \pi^*$ , 354 (4696) $n \rightarrow \pi^*$ ,<br>464(4419) CT, 677 d-d  | 634(12.84)                     | 317      |
| 8 | 317 (5411) $\pi \rightarrow \pi^*$ , 352 (4252) $n \rightarrow \pi^*$ ,<br>423(4379) , 469 (4342) CT, 685 d-d                           | No fluorescence                | 317, 352 |

Metallomacrocyclic xanthate complex **2** and metallomacrocyclic *N,O*- Schiff base complexes **6-7** clearly displayed (M+H) molecular ion peaks along with the other fragmentation peaks. (Supporting Information) The instability of **1-4** in solution limited our attempts to obtain single crystals suitable for single crystal XRD study. The powder X-ray diffraction study was performed on representative compounds (**K<sub>2</sub>xan<sup>1</sup>**, **1**, **3**, **5** and **7**) to understand features like crystal lattice and lattice parameters. The powder XRD data have been indexed and refined applying least square refinement by commonly used<sup>32</sup> program ‘POWDERX’<sup>33</sup> (Supporting Information). Notably, the results of PXRD analysis for xanthate ligand **K<sub>2</sub>xan<sup>1</sup>** and its Co<sup>II</sup>/Cu<sup>II</sup> complexes **1/3** as well as their corresponding Schiff base complexes **5/7** suggest their different packing patterns in the solid state. The indexing of powder XRD data for **5** and **7** gave the lattice system similar to that obtained from single crystal data with the differences in cell parameters probably arising due to the involvement of solvent of crystallization.

Further, geometry optimization for representative compounds **L<sup>1</sup>**, **K<sub>2</sub>xan<sup>1</sup>**, binuclear xanthate macrocycles **1**, **3** and their corresponding binuclear Schiff base macrocyclic derivatives **5**, **7** was performed using DFT study. (Supporting Information) Optimized geometry of **K<sub>2</sub>xan<sup>1</sup>** gives the required orientation of xanthate moieties essential for the

formation of metallomacrocyclic xanthate complexes **1-4**. The calculated structural parameters for complex **5** and **7** are comparable to their structural parameters obtained from X-ray crystallography (Supporting Information). The calculated HOMO-LUMO gaps are comparable to the experimental UV-visible absorption data (Table S6) and further validate the computed data as well as optimized structures.

The UV-visible absorption ( $10^{-4}$  M DMSO solution) and emission ( $10^{-4}$  M DMSO solution) properties of **L**<sup>1</sup>-**L**<sup>2</sup>, **K**<sub>2</sub>**xan**<sup>1</sup>-**K**<sub>2</sub>**xan**<sup>2</sup> and **1-8** were investigated at room temperature (Table 1 and Figure S21-S22). The electronic spectra of **1-8** clearly revealed the structural changes in xanthate and Schiff base complexes. The shorter absorption band ~315 nm is assigned to  $\pi \rightarrow \pi^*$  (phenyl) transitions and the longer absorption band ~360 nm is assigned to  $n \rightarrow \pi^*$  (imine) transitions whereas the absorption bands appeared in 400-490 nm regions are attributable to the intraligand charge transfer transitions in respective compounds.

Evidently, imine  $n \rightarrow \pi^*$  transition bands of **L**<sup>1</sup>, **L**<sup>2</sup> remain unaffected in corresponding xanthate ligands **K**<sub>2</sub>**xan**<sup>1</sup>, **K**<sub>2</sub>**xan**<sup>2</sup> and binuclear xanthate complexes **1-4**. However, a distinguishable blue shift of this transition band by 10-15 nm in the binuclear *N,O*-Schiff base complexes **5-8** was observed which clearly underlines the participation of imine moiety in the complex formation. The fluorescence spectra of **L**<sup>1</sup> and **K**<sub>2</sub>**xan**<sup>1</sup> display weak emission bands at 432, 513 and 520 nm upon excitation at  $\lambda_{ex}$  360 and 318 nm, respectively. However, **L**<sup>2</sup> and **K**<sub>2</sub>**xan**<sup>2</sup> display strong emission bands at 519 and 532 nm upon excitation at  $\lambda_{ex}$  318 and 497 nm respectively with a significant Stokes shift. Among **1-8**, complex **5** fluoresced with maximum emission at 410 nm upon excitation at  $\lambda_{ex}$  314 with a concomitant Stokes shift of  $\approx$  138 nm. Expectedly, all the Cu<sup>II</sup> complexes display no significant fluorescence properties, as Cu<sup>II</sup> is a well known fluorescence quencher.<sup>34</sup>

### Crystallographic Study

Complexes **5-8** have crystallized in orthorhombic *Pbca* (**5**), monoclinic *P2<sub>1</sub>/c* (**6**), orthorhombic *Pbca* (**7.DMSO**), monoclinic *C2/c* (**7.2CH<sub>2</sub>Cl<sub>2</sub>**) and monoclinic *P2<sub>1</sub>/c* (**8.CHCl<sub>3</sub>.8H<sub>2</sub>O**) centrosymmetric space groups. The X-ray crystal structures show one complete molecule in their asymmetric units, except **7.2CH<sub>2</sub>Cl<sub>2</sub>** and **8.CHCl<sub>3</sub>.8H<sub>2</sub>O** which contains half and two complete molecules in their asymmetric units, respectively. All the five compounds contain voids which are occupied by disordered solvent molecules in their crystal lattice, compound **5** and compound **6** have voids space which can be accounted for four water molecules each per unit cell respectively. A satisfactory disorder model for the solvent was not found in both of these cases, therefore the OLEX2 Solvent Mask routine (similar to PLATON/SQUEEZE) was used to mask out the disordered density. However, each asymmetric units of Compound **7.DMSO** has one DMSO molecule, compound **7.2CH<sub>2</sub>Cl<sub>2</sub>** has one *CH<sub>2</sub>Cl<sub>2</sub>* molecule and compound **8.CHCl<sub>3</sub>.8H<sub>2</sub>O** has one *CHCl<sub>3</sub>* molecule and eight water molecules respectively. The crystal structure of compound **8.CHCl<sub>3</sub>.8H<sub>2</sub>O** is obtained from poor quality data ought to weakly diffracting crystals and our efforts to get best diffraction quality crystals have been failed and we report this structure only for connectivity purpose. The reported structure is refined isotopically except Cu and its four connecting atoms and chlorine atoms of *CHCl<sub>3</sub>* solvent. The *ORTEP* view at 40 % probability for these complexes is shown in Fig. 1a-e. Details about data collection, refinement, and structure solution are recorded in Table S2, and the selected geometrical parameters are provided in Table S3.

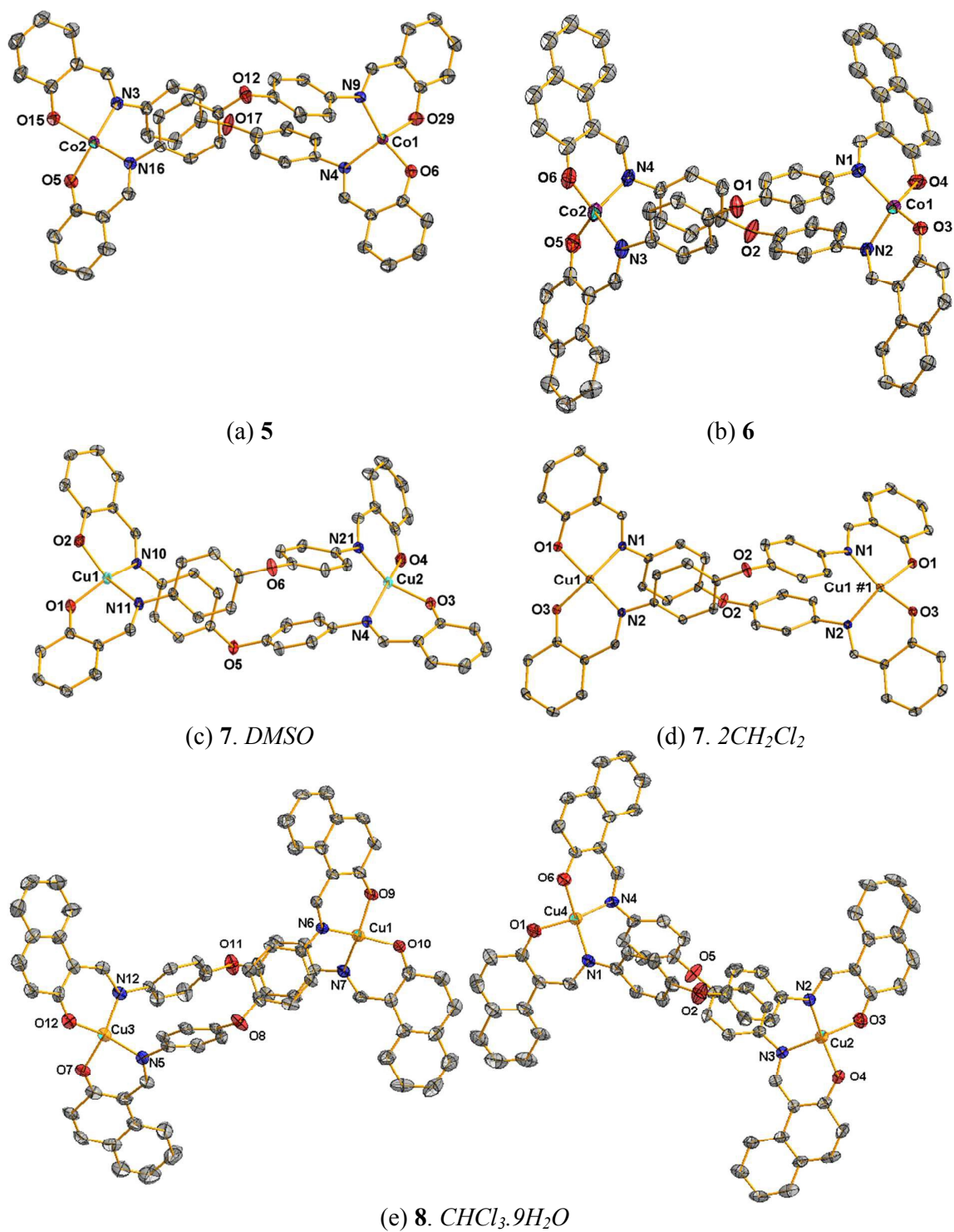


**Fig. 1** ORTEP diagram with atoms labelled showing 40% probability ellipsoids for (a) **5**, (b) **6**, (c) **7.DMSO**, (d) **7.2CH<sub>2</sub>Cl<sub>2</sub>** and (e) **8.CHCl<sub>3</sub>.8H<sub>2</sub>O**. Hydrogens and disordered solvent molecules are removed for clarity.

In **5-8**, each of the Co<sup>II</sup>/ Cu<sup>II</sup> centers are bonded to the available coordination sites of **L**<sup>1</sup> and **L**<sup>2</sup> through two imine nitrogen and two phenolic oxygen atoms. While the angles between the two O–M–N planes deviate largely from coplanarity, the O–M–O, and N–M–N angles differ significantly from 90° in all the molecules. The geometry around the metal ions in these complexes is thus essentially distorted tetrahedral. It appears that M–O and M–N bond lengths around one metal center in the binuclear Co<sup>II</sup> complexes **5, 6** is comparable with the similar distances around other metal center whereas these distances deviate significantly in the binuclear Cu<sup>II</sup> complex **7** (Table S3). It is noteworthy that the Co–O (1.884-1.908 Å) and Co–N (1.954-1.988 Å) bond distances in binuclear Co<sup>II</sup> complexes **5-6** are significantly longer than the similar distances observed in the planar Schiff base Co<sup>II</sup> complex (1.835-1.847 Å for Co–O and 1.861-1.864 Å for Co–N).<sup>35</sup> However, longer Cu–O (1.888-1.976 Å) and shorter Cu–N (1.949-1.982 Å) distances, compared to planar Schiff base Cu<sup>II</sup> complex (1.874 Å for Cu–O and 2.009 Å for Cu–N) were observed.<sup>36</sup> However, these distances are indeed consistent with the similar measurements observed in analogous tetrahedral Cu<sup>II</sup> complex reported earlier.<sup>27a</sup> In all the binuclear complexes, the etheral bond angle of one linker appeared in the normal range<sup>23</sup> (117.5-118.0°) whereas significant shrinking of a similar angle (115.4-116.4°) associated with the other linker was observed. This inward bending of the diphenyl ether linkers suggests flexibility of the coordinated ligands, essential for the formation of macrocyclic structures. In addition, the unique coordination geometry adopted by Co<sup>II</sup> or Cu<sup>II</sup> ions and the presence of two arc shaped ligands form double helical molecular unit of **5-8** as exemplified in Fig. 2.

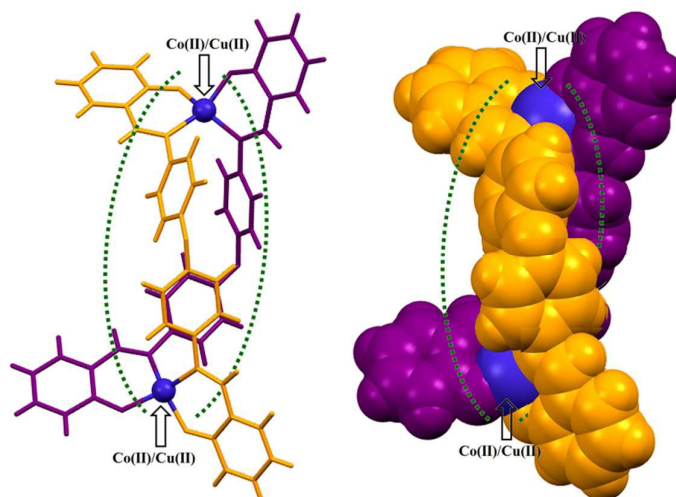


**Fig. 2** General representation of double helical molecular unit formed in complexes **5-8**.

Further, single-crystal X-ray diffraction data is useful in revealing the supramolecular structures of **5-8** and also in gauging the crucial role of aromatic moieties present in the molecular framework and that of solvent molecules on the association of molecules in the solid state. The study revealed that the presence of phenyl/naphthyl rings and solvent molecules induces electronic and conformational changes (dihedral angles) that apparently modify the nature and number of donor-acceptor sites for noncovalent interactions such as  $\pi\cdots\pi$ ,  $\text{CH}\cdots\pi$ ,  $\text{CH}\cdots\text{O}$ ,  $\text{Cl}\cdots\text{O}$  and/ or  $\text{O}\cdots\text{S}$ , leading to diverse crystal packing patterns. Relevant discussion on significant non-conventional intermolecular interactions observed in **5-8** is summarized in the supporting information.

### ***In vitro* anticancer activity**

All the compounds **L**<sup>1</sup>, **L**<sup>2</sup>, **K<sub>2</sub>xan**<sup>1</sup>, **K<sub>2</sub>xan**<sup>2</sup>, **1-8** were screened against the malignant cell lines HEP 3B and IMR 32 for their *in vitro* cytotoxicity by the MTT assay.<sup>37</sup> The cytotoxicity of these compounds were compared with the clinically used antineoplastic drug cisplatin and lead compound 4,4'-diaminodiphenyl ether (**L**). The 50% inhibition concentration ( $\text{IC}_{50}$ ) values obtained after incubation for all the compounds against HEP 3B (6 h) and IMR 32 (14 h) are summarized in Table 2, Fig. 3.

**Table 2** *In vitro* cytotoxicity MTT assay  $IC_{50}$  ( $\mu M$ ) for entry 1-16 against HEP 3B and IMR 32 cancer cell lines.

| Entry          | Compound                        | Antitumor activity ( $IC_{50}$ values) <sup>b</sup> |                               |
|----------------|---------------------------------|---|-------------------------------|
|                |                                 | HEP 3B $\mu M$ (1mL) $\pm SE$                       | IMR 32 $\mu M$ (1mL) $\pm SE$ |
| 1 <sup>a</sup> | L                               | 415.4 $\pm$ 2.2                                     | 272.4 $\pm$ 2.4               |
| 2              | L <sup>1</sup>                  | 137.8 $\pm$ 13.9                                    | 104.0 $\pm$ 3.3               |
| 3              | L <sup>2</sup>                  | 36.7 $\pm$ 5.0                                      | 166.9 $\pm$ 11.1              |
| 4              | K <sub>2</sub> xan <sup>1</sup> | 17.8 $\pm$ 2.9                                      | 23.2 $\pm$ 1.4                |
| 5              | K <sub>2</sub> xan <sup>2</sup> | 79.5 $\pm$ 6.1                                      | 26.2 $\pm$ 1.3                |
| 6              | 1                               | 52.9 $\pm$ 1.3                                      | 51.8 $\pm$ 2.9                |
| 7              | 2                               | 54.4 $\pm$ 0.3                                      | 64.4 $\pm$ 3.8                |
| 8              | 3                               | 8.1 $\pm$ 0.8                                       | 1.8 $\pm$ 0.3                 |
| 9              | 4                               | 8.8 $\pm$ 1.7                                       | 7.3 $\pm$ 0.6                 |
| 10             | 5                               | 69.7 $\pm$ 3.6                                      | 99.7 $\pm$ 6.6                |
| 11             | 6                               | 43.4 $\pm$ 4.7                                      | 50.17 $\pm$ 2.5               |
| 12             | 7                               | 19.2 $\pm$ 2.1                                      | 13.27 $\pm$ 1.1               |
| 13             | 8                               | 14.3 $\pm$ 1.3                                      | 28.8 $\pm$ 1.4                |
| 14             | Co <sup>II</sup>                | 290.9 $\pm$ 4.1                                     | 343.2 $\pm$ 17.1              |
| 15             | Cu <sup>II</sup>                | 42.9 $\pm$ 4.3                                      | 19.0 $\pm$ 2.9                |
| 16             | Cisplatin                       | 74.6 $\pm$ 1.3                                      | 107.9 $\pm$ 0.3               |

(<sup>a</sup>:  $IC_{50}$  value retrieved from ref<sup>22</sup>; <sup>b</sup>: The data are expressed as  $\mu M$  concentration and value represents the average of three sets of independent experiments.)

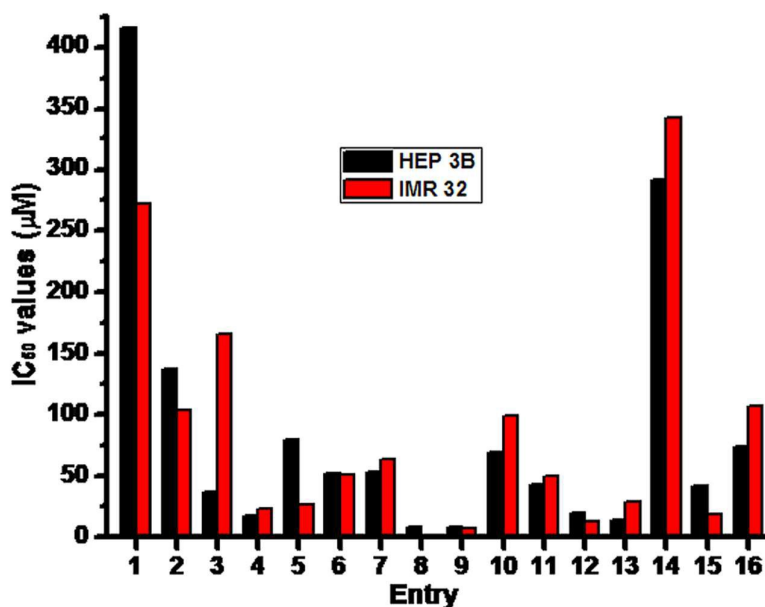


**Fig. 3** *In vitro* cytotoxicity ( $IC_{50}$ ) for entries 1-16 against malignant HEP 3B and IMR 32 cells.

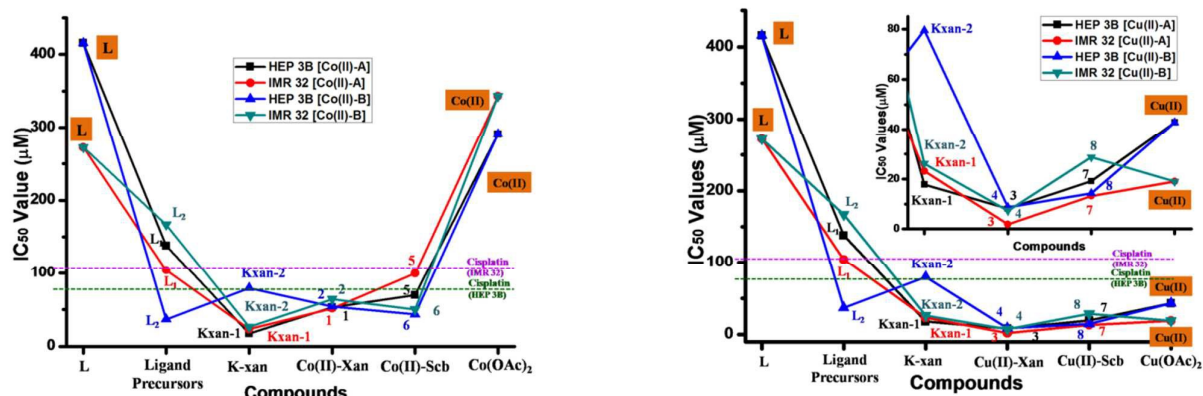


**Fig. 4** Effect of functionality changes on *in vitro* cytotoxicity against HEP 3B and IMR 32 cells.

The condensation of salicylaldehyde with lead compound **L** resulted into **L**<sup>1</sup> with a  $\approx$  3 fold increase in the cytotoxicity ( $IC_{50}$ :  $137.8 \pm 13.9 \mu\text{M}$  against HEP 3B and  $104.0 \pm 3.3 \mu\text{M}$  against IMR 32). However, condensation of 2-hydroxy naphthaldehyde with **L** resulted into **L**<sup>2</sup> with  $>10$  and a two fold increase in the cytotoxicity against HEP 3B ( $36.7 \pm 5.0 \mu\text{M}$ ) and IMR 32 ( $166.9 \pm 11.0 \mu\text{M}$ ) cell lines, respectively. The cytotoxicity of **L**<sup>1</sup> and **L**<sup>2</sup> further augmented on the formation of their respective xanthate salts and ensuing complexes, particularly copper xanthate complexes. All binuclear xanthate complexes displayed comparable anticancer activity, except **3** which exhibits differential activity against both the cell lines. Interestingly, binuclear Cu<sup>II</sup>xanthate complexes were found extremely active against both the cell lines ( $IC_{50}$ :  $8.1 \pm 0.8 \mu\text{M}$  (**3**),  $8.8 \pm 1.7 \mu\text{M}$  (**4**) against HEP 3B and  $1.9 \pm 0.3 \mu\text{M}$  (**3**) and  $7.3 \pm 0.6 \mu\text{M}$  (**4**) against IMR 32) and this projects them as good candidates for being employed as potent antitumor agents. Unlike binuclear xanthate analogues, binuclear *N, O*-Schiff base complexes could not preserve the anticancer activity. Binuclear Cu<sup>II</sup> *N, O*-Schiff base complexes **7** and **8** exhibit 2-7 fold better potency than that of cobalt analogues **5**-**6**. The overall data suggests that **K**<sub>2</sub>**xan**<sup>1</sup>, **K**<sub>2</sub>**xan**<sup>2</sup>, and complex **1**-**8** are more cytotoxic against both the cell lines than the clinically used antineoplastic drug cisplatin (Table 2). In general, all the complexes bearing copper center are more potent compared to their cobalt bearing congeners probably due to the predominant favouring of the Cu<sup>II</sup> ion in biological

systems than that of  $\text{Co}^{\text{II}}$ . The probable mode of action leading to cell death at molecular level can be explained on the basis of several previously observed effects of isostructural dithiocarbamate complexes and complexes derived from *N, O*- donor ligands (Supporting Information). Among the investigated compounds,  $\text{L}^1$ ,  $\text{L}^2$ ,  $\text{K}_2\text{xan}^1$  and  $\text{K}_2\text{xan}^2$  can be classified as moderate cytotoxic agents, binuclear *N, O*-Schiff base analogues as good whereas binuclear xanthate complexes can be excellent cytotoxic agents; especially **3-4** with optimum cytotoxic ability (Fig. 4) against both the cell lines.

In analogy with the recent investigations,<sup>38</sup> we have calculated the stereo-electronic parameters such as highest occupied molecular orbital (HOMO), lowest unoccupied molecular orbital (LUMO) energies, dipole moment and charges on the N/O/S/M atoms using density functional theory (DFT). Calculated stereoelectronic parameters and experimental  $\text{IC}_{50}$  values against HEP 3B and IMR 32 cells for model compounds are summarized in Table S13. Among the model complexes **1**, **3** and **5**, **7** bearing similar ligand framework, complexes **3** and **7** with lower HOMO energy and lower dipole moment (greater lipophilicity) (Supporting Information) exhibit higher cytotoxicity, suggestive of higher bioavailability at the site of action and reactivity in the biological conditions. Notably, complex **3** bearing negative charge on copper and positive charges on sulfur atoms exhibits higher reactivity towards biological receptors, which could underline the extraordinary ability of **3** to arrest the cell growth against both the cell lines. These theoretical parameters correlate well with the experimental results since complex **3** is the most active against both the cell lines.

### Induction of Apoptosis

In higher organism, apoptosis is a key process for boy haemostasis during development, embryonic development, the immune system, and ageing. It is also known to play an important role in many pathological conditions like cancer and neurodegeneration.<sup>39</sup> Apoptotic cell death is postulated to be the crucial mechanism in natural tumor suppression

and cancer treatment, which abolish abnormal, malignant cells and reduce the tumor size.<sup>40</sup> Thus, it is important to develop novel chemical agents to specifically induce apoptosis for therapeutic purposes. In addition to the MTT assay, 'Flow Cytometry' is considered as the analytical tool for investigation of potency, not only for cell viability, but also to evaluate membrane and chromosomal damage, cell-cycle analysis and morphological changes. Hence, for quantification of the extent of apoptotic and necrotic cell death, flow cytometry studies were performed upon treatment of some representative compounds on **HEP 3B** and **IMR 32** cells. The flow-cytometric density plot (Figure S30) illustrates the induction of apoptosis in **HEP 3B** and **IMR 32** cells after the treatment with **K<sub>2</sub>xan<sup>1</sup>** and binuclear metallamacrocyclic complexes **1**, **3**, **6** and **7**.

With reference to Table 3, less than 1% live cell population was observed for both the cell lines after treatment which reinforced the extreme cytotoxicity of the compounds investigated by the MTT assay. Interestingly, the apoptotic cell populations *viz.* 32.1%, 70.2%, 13.5%, 62.3% 10.9% were observed for HEP 3B cells whereas 76.3%, 19.5%, 51.9%, 54.3% 1.2% were observed for the IMR 32 cells, after treating with **K<sub>2</sub>xan<sup>1</sup>**, **1**, **3**, **6** and **7**, respectively. It may be noted that 64.1% of pro-apoptotic HEP 3B cells were observed upon treatment with **K<sub>2</sub>xan<sup>1</sup>** whereas 77.3% and 43.2% of pro-apoptotic IMR 32 cell population was observed upon treatment with **1** and **3**, respectively.

**Table 3** Apoptotic/ necrotic population of HEP 3B and IMR 32 cells upon treatment with **K<sub>2</sub>xan<sup>1</sup>**, binuclear metallamacrocyclic complexes **1**, **3**, **6** and **7**.

| Sample                              | HEP 3B (%) |           |            |               | IMR 32(%) |           |            |               |
|-------------------------------------|------------|-----------|------------|---------------|-----------|-----------|------------|---------------|
|                                     | Necrotic   | Apoptotic | Live cells | Pro-apoptotic | Necrotic  | Apoptotic | Live cells | Pro-apoptotic |
| <b>K<sub>2</sub>xan<sup>1</sup></b> | 3.8        | 32.1      | 0.0        | 64.1          | 21.2      | 76.3      | 0.0        | 2.5           |
| <b>1</b>                            | 25.8       | 70.2      | 0.2        | 3.8           | 3.0       | 19.5      | 0.2        | 77.3          |
| <b>3</b>                            | 85.9       | 13.5      | 0.0        | 0.5           | 4.8       | 51.9      | 0.1        | 43.2          |
| <b>6</b>                            | 30.8       | 62.5      | 0.1        | 6.7           | 43.3      | 54.3      | 0.0        | 2.3           |
| <b>7</b>                            | 88.3       | 10.9      | 0.2        | 0.5           | 97.6      | 1.2       | 1.0        | 0.3           |
| Control                             | 0.1        | 0.0       | 99.8       | 0.1           | 0.1       | 0.0       | 99.7       | 0.2           |
| Cisplatin                           | 10.3       | 30.4      | 0.0        | 59.3          | ...       | ...       | ...        | ...           |

In particular, HEP 3B and IMR 32 cells treated with **7** and HEP 3B cells treated with **3**, predominantly dyed with propidium iodide and evident for the induction of necrosis to a

great extent, whereas IMR 32 cells treated with **6** showed simultaneous binding of annexin V and propidium iodide, indicative of the transition of apoptosis to necrosis (late apoptosis and secondary necrosis).<sup>41</sup> Apoptosis inducing ability of compounds **K<sub>2</sub>xan<sup>1</sup>**, **1** and **6** is clearly reflected by the sum of apoptotic and pro-apoptotic cell populations (96.2%, 74% and 69.2% for HEP 3B; 78.8%, 96.8% and 56.6% for IMR 32) of treated cells. The distinct behavior of the binuclear metallomacrocyclic xanthate complex **3** towards both the cell lines is also reflected by the sum of apoptotic and pro-apoptotic cell populations of 95.1% (IMR 32) and 14% (Hep 32). The differential apoptotic, pro-apoptotic and necrotic cell populations in treated HEP 3B and IMR 32 cells is indicative of the involvement of different receptors in the cytotoxicity.

## Conclusion

A metathetical reaction of 4,4'-bis(2-dithiocarbonatobenzylideneamino)diphenyl ether (**xan<sup>1</sup>**) or 4,4'-bis(2-dithiocarbonatonaphthylmethylideneamino)diphenyl ether (**xan<sup>2</sup>**) with Co<sup>II</sup> or Cu<sup>II</sup> acetates in Et<sub>3</sub>N affords access to novel series of phenolate based binuclear Co<sup>II</sup> or Cu<sup>II</sup> xanthate metallomacrocyclic complexes of the type [M<sub>2</sub>-μ<sup>2</sup>-bis-(κ<sup>2</sup>S,S-xan<sup>1</sup>/xan<sup>2</sup>)] (**1-4**). These metastable products undergo a facile transformation into [2:2] binuclear *N*, *O*-Schiff base macrocycles of the type [M<sub>2</sub>-μ<sup>2</sup>-bis-(κ<sup>2</sup>N,*O*-L<sup>1</sup>/ L<sup>2</sup>)] (L<sup>1</sup> = 4,4'-bis(2-hydroxybenzylideneamino)diphenyl ether, L<sup>2</sup> = 4,4'-bis(2-hydroxynaphthylmethylideneamino)diphenyl ether) **5-8**. The unique coordination geometry of metal ions together with the arc shaped ligands form double helical molecular unit of **5-8**. Interestingly, the binuclear metallamacrocyclic **3** was found to be the most active against the human cancer cells and the cytotoxicity data confirms better potency of all the investigated compounds than the reference drug "cisplatin". These scaffolds, with excellent IC<sub>50</sub> values were explored as a novel class of active chemical agents to induce apoptosis, required for a major therapeutic implication in cancer therapy. Owing to the unique characteristics of macrocyclic scaffolds and considering

the advantage of their bioavailability, versatile coordination ability and the ability to change their oxidation state (in case of copper/ cobalt centers) these binuclear macrocyclic complexes project themselves as efficacious anticancer agents.

## Experimental Section

### Materials

All the synthetic manipulations were performed under nitrogen atmosphere. The solvents were of laboratory grade available at various commercial sources and distilled prior to use by following the standard procedures. 4,4'-diaminodiphenyl ether (99%) (National Chemicals), potassium hydroxide, carbon disulfide (99%), metal acetates such as  $\text{Co}(\text{OAc})_2 \cdot 4\text{H}_2\text{O}$  and  $\text{Cu}(\text{OAc})_2 \cdot \text{H}_2\text{O}$  (all Merck), 2-hydroxybenzaldehyde (98%), 2-hydroxynaphthaldehyde (98%) (Chemlabs) were used as received. Ligand precursors 4,4'-bis(2-hydroxybenzylideneamino) diphenyl ether ( $\text{L}^1$ ) and 4,4'-bis(2-hydroxynaphthylmethylideneamino)diphenyl ether ( $\text{L}^2$ ) were synthesized following literature procedure.<sup>23</sup>

### Instrumentation

IR (KBr pellets) spectra were recorded in the 4000-400  $\text{cm}^{-1}$  range using a Perkin-Elmer FTIR Spectrometer. The NMR spectra were obtained on a Bruker 400 MHz spectrometer in DMSO- $d_6$  unless otherwise noted. Elemental analyses were performed on a Perkin-Elmer Series II CHNS/O Analyzer 2400. Mass spectra were obtained on a Thermo Scientific DSQ-II and AB SCIEX 3200 Q TRAP LC/MS/MS system. Single crystal X-ray analysis was carried out on Agilent's Gemini diffractometer equipped with a Eos CCD detector. UV-visible spectra were recorded on a Perkin Elmer Lambda 35 UV-vis spectrophotometer. TGA/DTA plots were obtained using SII TG/DTA 6300 in flowing  $\text{N}_2$  with a heating rate of 10  $^\circ\text{C min}^{-1}$ . GC analysis was carried out on CLARUS500, PE AutoSystem type GC equipped with FID detector. Powder X-ray diffraction studies were performed on a 'X

Calibur, Eos, Gemini' X-ray diffractometer using Cu source, CrysAlisPro data reduction: Agilent Technologies Version 1.171.37.33 program(s) was used to process the data and the 'POWDERX' program for indexing the powder XRD data. Flow cytometry studies were performed on Fluorescent Activated Cell Sorter (FACS) analyzer with high speed sorter model BD FACS Aria III.

### General procedure for synthesis of xanthate salts $\mathbf{K_2xan^1}$ and $\mathbf{K_2xan^2}$

To a solution of KOH (2.5 mmol, 141 mg) in 25 ml distilled water, 4,4'-bis(2-hydroxyarylmethylideneamino)diphenyl ether precursors  $\mathbf{L^1}$  (1 mmol, 408 mg) or  $\mathbf{L^2}$  (1 mmol, 508 mg) was added with stirring. After 15 minutes, an excess amount of  $\text{CS}_2$  (2 ml) was added and the reaction was allowed to continue at room temperature for 12 h. The solvent was evaporated under vacuum and solid was washed with diethyl ether to yield the product  $\mathbf{K_2xan^1}$  or  $\mathbf{K_2xan^2}$ . The compound was dried under vacuum, stored under a nitrogen atmosphere and samples were taken for analysis. This reaction is outlined in Scheme 1.

**$\mathbf{K_2[4,4'-bis(2-dithiocarbonatobenzylideneamino)diphenyl ether]}$  ( $\mathbf{K_2xan^1}$ ).** Yellow solid; Yield: *ca* 624 mg, 98%; Melting/Decomposition point: 205-210 °C. Anal. Calcd for  $[\text{C}_{28}\text{H}_{18}\text{K}_2\text{N}_2\text{O}_3\text{S}_4]$ : C, 52.80; H, 2.85; N, 4.40. Found: C, 52.87; H, 2.95; N, 4.49. IR (KBr pellet,  $\text{cm}^{-1}$ ): 1620s  $\nu(\text{C}=\text{N})$ , 1148s, 1109m  $\nu(\text{C}-\text{O})$ , 1031w, 996s, 982m  $\nu(\text{CS}_2)$ .  $^1\text{H}$  NMR (400 MHz, DMSO- $d_6$ ): ( $\delta$  from TMS) 6.880(m, 4*H-Ph*), 7.110(d, 4*H-Ph*), 7.354(m, 2*H-Ph*), 7.44(d, 4*H-Ph*), 7.645(dd, 2*H-Ph*), 8.97(s, 2*H-N=CH*).  $^{13}\text{C}$  NMR (400 MHz, DMSO- $d_6$ ): ( $\delta$  from TMS) 115.24, 115.34, 117.57, 119.38, 119.93, 121.42, 123.19, 123.50, 124.36, 127.61, 133.38, 135.63, 144.54, 146.12, 148.93, 158.45 (*all corresponds to Ph*), 162.02 ( $-\text{N}=\text{CH}$ ), 190.86( $-\text{CS}_2$ ).

**$\mathbf{K_2[4,4'-bis(2-dithiocarbonatonaphthylmethylideneamino)diphenyl ether]}$  ( $\mathbf{K_2xan^2}$ ).** Dark yellow solid; Yield: *ca* 722 mg, 98%; Melting/Decomposition point: 180-185 °C decomposes. Anal. Calcd for  $[\text{C}_{36}\text{H}_{22}\text{K}_2\text{N}_2\text{O}_3\text{S}_4]$ : C, 58.67; H, 3.01; N, 3.80. Found: C, 58.08;

H, 3.12; N, 3.85. IR (KBr pellet,  $\text{cm}^{-1}$ ): 1624s  $\nu(\text{C}=\text{N})$ , 1140s, 1084m  $\nu(\text{C}-\text{O})$ , 1038w, 998s, 970m  $\nu(\text{CS}_2)$ .  $^1\text{H}$  NMR (400 MHz, DMSO- $d_6$ ): ( $\delta$  from TMS) 7.05(dd, 2*H-Ph*), 7.18(dd, 4*H-Ph*), 7.36(t, 2*H-Ph*), 7.545(m, 2*H-Ph*), 7.71(dd, 4*H-Ph*), 7.8(d, 2*H-Ph*), 7.93(d, 2*H-Ph*), 8.525(d, 2*H-Ph*), 9.688(s, 2*H-N=CH*).  $^{13}\text{C}$  NMR (400 MHz, DMSO- $d_6$ ): ( $\delta$  from TMS) 109.14, 118.85, 118.91, 120.10, 120.92, 122.21, 122.72, 122.93, 123.90, 123.95, 127.19, 128.49, 129.44, 133.51, 136.88, 140.63, 155.69, 156.29 (*all corresponds to Ph*), 169.62 ( $-\text{N}=\text{CH}$ ), 190.24 ( $-\text{CS}_2$ ).

#### General procedure for synthesis of 1-4

To a solution of xanthate ligand  $\text{K}_2\text{xan}^1$  (0.5 mmol, 318.45 mg) or  $\text{K}_2\text{xan}^2$  (0.5 mmol, 368.51mg) in 20 ml of distilled  $\text{Et}_3\text{N}$ ,  $\text{Co}(\text{OAc})_2 \cdot 4\text{H}_2\text{O}$  /  $\text{Cu}(\text{OAc})_2 \cdot \text{H}_2\text{O}$  (0.6 mmol, 149.45 mg) / (0.6 mmol, 119.79 mg) was added with rigorous stirring (Scheme 2). The reaction was allowed to continue for 12h. The solid residue was filtered and washed with  $\text{Et}_3\text{N}$  followed by distilled water and hexane to yield the products **1-4**. These products were dried under high vacuum, stored under a nitrogen atmosphere and samples were taken for analysis.

**[Co<sub>2</sub>- $\mu^2$ -bis-( $\kappa^2\text{S},\text{S-xan}^1$ )] (1)**. Buff solid; Yield: *ca* 305 mg, 99%; Melting/Decomposition point: 180-185 °C. Anal. Calcd for  $[\text{C}_{56}\text{H}_{36}\text{Co}_2\text{N}_4\text{O}_6\text{S}_8]$ : C, 54.45; H, 2.94; N, 4.54; S, 20.77. Found: C, 54.12; H, 3.05; N, 4.50; S, 20.75. IR (KBr pellet,  $\text{cm}^{-1}$ ): 1620s  $\nu(\text{C}=\text{N})$ , 1152m, 1112m, 1104m  $\nu(\text{C}-\text{O})$ , 1031w, 1012w, 983m  $\nu(\text{CS}_2)$ .

**[Co<sub>2</sub>- $\mu^2$ -bis-( $\kappa^2\text{S},\text{S-xan}^2$ )] (2)**. Orange solid; Yield: *ca* 344 mg, 96%; Melting/Decomposition point: 200-205 °C. Anal. Calcd for  $[\text{C}_{72}\text{H}_{44}\text{Co}_2\text{N}_4\text{O}_6\text{S}_8]$ : C, 60.24; H, 3.09; N, 3.90; S, 17.87. Found: C, 60.25; H, 3.21; N, 3.85; S, 17.70. Mass (MS ES<sup>+</sup>): 1436.1 (M+H). IR (KBr pellet,  $\text{cm}^{-1}$ ): 1616s, 1615s, 1601s  $\nu(\text{C}=\text{N})$ , 1145m, 1110m  $\nu(\text{C}-\text{O})$ , 1041w, 1012m, 980m  $\nu(\text{CS}_2)$ .

**[Cu<sub>2</sub>- $\mu^2$ -bis-( $\kappa^2\text{S},\text{S-xan}^1$ )] (3)**. Brown solid; Yield: *ca* 305 mg, 98%; Melting/Decomposition point: 160-165 °C. Anal. Calcd for  $[\text{C}_{56}\text{H}_{36}\text{Cu}_2\text{N}_4\text{O}_6\text{S}_8]$ : C, 54.04; H, 2.92; N, 4.50; S, 20.61. Found: C, 54.10; H, 2.99; N, 4.55; S, 20.91. IR (KBr pellet,  $\text{cm}^{-1}$ ): 1614s  $\nu(\text{C}=\text{N})$ , 1149s,

1127m, 1104m  $\nu(\text{C-O})$ , 1029w, 1010m, 982w  $\nu(\text{CS}_2)$ .

**[Cu<sub>2</sub>- $\mu^2$ -bis-( $\kappa^2\text{S,S-xan}^2$ )] (4).** Brown solid; Yield: *ca* 336 mg; 93% Melting/Decomposition point: 100-105 °C. Anal. Calcd for [C<sub>72</sub>H<sub>44</sub>Cu<sub>2</sub>N<sub>4</sub>O<sub>6</sub>S<sub>8</sub>]: C, 59.86; H, 3.07; N, 3.88; S, 17.76. Found: C, 59.23; H, 3.35; N, 3.72; S, 17.91. IR (KBr pellet,  $\text{cm}^{-1}$ ): 1617s, 1602s  $\nu(\text{C=N})$ , 1142m, 1103m  $\nu(\text{C-O})$ , 1041w, 1011w, 982w, 967w  $\nu(\text{CS}_2)$ .

**General procedure for synthesis of 5-8.** Binuclear metallomacrocyclic xanthate complexes (0.5 mmol) **1** (617.65 mg), **2** (717.67 mg), **3** (622.26 mg) or **4** (722.38 mg) were dissolved in dichloromethane and volatiles were allowed to evaporate at room temperature (Scheme 2). The brownish **5** and **6** (in case of **1** and **2**) and blackish brown **7** and **8** (in case of **3** and **4**) crystalline solids obtained, were washed with diethyl ether for three times. Solids were dried under vacuum to yield corresponding binuclear metallomacrocyclic bis-*N,O*-Schiff base complexes **5-8**; products were stored under a nitrogen atmosphere and samples were taken for analysis.

**[Co<sub>2</sub>- $\mu^2$ -bis-( $\kappa^2\text{N,O-L}^1$ )] (5).** Pale brown solid, Yield: *ca* 377 mg, 81%; Melting/Decomposition point: 170-175 °C. Anal. Calcd for [C<sub>52</sub>H<sub>36</sub>Co<sub>2</sub>N<sub>4</sub>O<sub>6</sub>]: C, 67.10; H, 3.90; N, 6.02. Found: C, 67.20; H, 3.95; N, 5.96. IR (KBr pellet,  $\text{cm}^{-1}$ ): 1608s, 1584s  $\nu(\text{C=N})$ .

**[Co<sub>2</sub>- $\mu^2$ -bis-( $\kappa^2\text{N,O-L}^2$ )] (6).** Dark brown solid, Yield: *ca* 526 mg, 93%; Melting/Decomposition point: 200-205 °C. Anal. Calcd for [C<sub>68</sub>H<sub>44</sub>Co<sub>2</sub>N<sub>4</sub>O<sub>6</sub>]: C, 72.22; H, 3.92; N, 4.95. Found: C, 72.18; H, 4.05; N, 4.91. Mass (MS ES<sup>+</sup>): 1131.0 (M+H). IR (KBr pellet,  $\text{cm}^{-1}$ ): 1616s, 1601s  $\nu(\text{C=N})$ .

**[Cu<sub>2</sub>- $\mu^2$ -bis-( $\kappa^2\text{N,O-L}^1$ )] (7).** Blackish brown solid; Yield: *ca* 423 mg, 90 %; Melting/Decomposition point: 200-205 °C. Anal. Calcd for [C<sub>52</sub>H<sub>36</sub>Cu<sub>2</sub>N<sub>4</sub>O<sub>6</sub>.CH<sub>2</sub>Cl<sub>2</sub>]: C, 62.11; H, 3.74; N, 5.47. Found: C, 62.13; H, 3.75; N, 5.45. Mass (MS ES<sup>+</sup>): 931 (M+H). IR (KBr pellet,  $\text{cm}^{-1}$ ): 1617s, 1602s  $\nu(\text{C=N})$ .

[Cu<sub>2</sub>-μ<sup>2</sup>-bis-(κ<sup>2</sup>N,O-L<sup>2</sup>)] (**8**). Blackish brown solid; Yield: *ca* 542 mg, 95 %; Melting/Decomposition point: 150-155 °C. Anal. Calcd for [C<sub>68</sub>H<sub>44</sub>Cu<sub>2</sub>N<sub>4</sub>O<sub>6</sub>]: C, 71.63; H, 3.89; N, 4.91. Found: C, 71.60; H, 3.95; N, 4.89. IR (KBr pellet, cm<sup>-1</sup>): 1616s, 1603s ν(C=N).

### X-ray structure determinations

Single crystals suitable for X-ray crystallographic study were obtained by slow evaporation of dichloromethane solution of **5-7** at 4 °C and a chloroform solution of **8**. The crystals of **7** were also grown by the slow diffusion of hexane in a DMSO solution in order to explore the solvent effect on crystallization and thus its impact on supramolecular packing in the solid state. The intensity data for **5** [C<sub>52</sub>H<sub>36</sub>Co<sub>2</sub>N<sub>4</sub>O<sub>6</sub>], **7.DMSO** [C<sub>54</sub>H<sub>40</sub>Cu<sub>2</sub>N<sub>4</sub>O<sub>7</sub>S], **7.2CH<sub>2</sub>Cl<sub>2</sub>** [C<sub>54</sub>H<sub>40</sub>Cl<sub>4</sub>Cu<sub>2</sub>N<sub>4</sub>O<sub>6</sub>] and **8.CHCl<sub>3</sub>.9H<sub>2</sub>O** [C<sub>137</sub>H<sub>105</sub>Cl<sub>3</sub>Cu<sub>4</sub>N<sub>8</sub>O<sub>22</sub>] was collected on Oxford X Calibur and Gemini diffractometer respectively equipped with Eos CCD detector at 298 K. Monochromatic Cu-Kα (λ = 1.54184) (in case of **5**) and Mo-Kα X-ray (λ=0.71073 Å) (in case of **7-8**) radiations were used for the measurements. Data was collected and reduced by using the “CrysAlispro” program (Version 1.171.37.33 Agilent Technologies, 2014).<sup>42a</sup> Intensity data for **6** [C<sub>68</sub>H<sub>44</sub>Co<sub>2</sub>N<sub>4</sub>O<sub>6</sub>] were collected on a Bruker Smart Apex CCD diffractometer using graphite-monochromated Mo-Kα radiation (λ= 0.71073 Å). The data integration and reduction were processed with SAINT<sup>42b</sup> software. An empirical absorption correction was applied to the collected reflections with SADABS.<sup>42c</sup> All the crystal structure were solved by the direct methods, and the refinement was carried out by full-matrix least squares against *F*<sup>2</sup> using SHELXL-97 program package<sup>43</sup> and Olex2 (version 1.2.5) program package.<sup>44</sup> MASK procedure of Olex2 is used to treat the disordered solvent molecules in each structure. All non-hydrogen atoms were refined anisotropically.

### In vitro cytotoxic study

**Cell line and culture.** Hepatoma (HEP 3B) and Neuroblastoma (IMR 32) cell lines were procured from the National Center for Cell Science, Pune. Dubecoos Modified Essential Medium (DMEM) and Foetus Bovine Serum (FBS) were procured from HiMedia whereas cisplatin from Sigma Aldrich. The human cell lines HEP 3B and IMR 32 were established in DMEM with 10% FBS in humidified atmosphere supplied with 5% CO<sub>2</sub> at 37 °C. The IMR 32 cell line was differentiated as a neuron by using sodium butyrate for 9 days of incubation at 37°C at a concentration of 5% CO<sub>2</sub>. The compounds reported in this article were screened for their antitumor activity against both the cell lines at varying concentration.

**MTT assay for cell viability/ proliferation.** The cell growth inhibition was determined by MTT assay with some modifications.<sup>37</sup> Schiff base precursors (**L<sup>1</sup>**, **L<sup>2</sup>**), xanthate ligands (**K<sub>2</sub>xan<sup>1</sup>**, **K<sub>2</sub>xan<sup>2</sup>**), binuclear xanthate complexes (**1-4**) and binuclear Schiff base complexes (**5-8**) were dissolved in DMSO and then diluted with water. The content of DMSO in each sample was 1%. Cells were seeded in 96-well plates at a density of  $1 \times 10^3$  cells per well and incubated for 24 h. These cells were treated with different concentrations of compounds reported in this paper for 6 h (against HEP 3B) and 14 h (against IMR 32). Cisplatin was also screened against both the cell lines under similar experimental conditions. After removal of the media, the culture was incubated with 20  $\mu$ L of media containing 5 mg/ml stock solution of MTT in PBS and 60  $\mu$ L of DMEM for 6 h at 37 °C in 5% CO<sub>2</sub> incubator. Formazan crystal formed by metabolically viable cells were dissolved in DMSO and the optical density was measured at 570 nm by ELISA reader (METERTECH- $\Sigma$ 960). The number of viable cells was proportional to the extent of formazan production.

**Statistical Analysis for Determination of IC<sub>50</sub>.** Six sets of each sample were screened and the data obtained, was analyzed in Prism/OriginPro 8 for standard error and probit analysis. The percent cytotoxicity index (% CI) was as follows:

% CI=  $[1 - (\text{OD of treated cells}/\text{OD of control cells})] \times 100$  % (where, CI= cytotoxicity index, OD= optical density.)

A plot of % CI versus concentration was obtained from the experimental data for each set of experiments. IC<sub>50</sub> values (50% growth inhibition of cell) were determined from the graph. Each test was repeated thrice and the results were expressed as mean IC<sub>50</sub> ± SD.

**Annexin V/PI Double Staining for Cell Death Analysis.** The cell death assessment was performed using annexin V alexa Fluro 4888 and propidium iodide apoptosis kit, procured from Himedia. For apoptosis measurement, HEP 3B and IMR 32 cells ( $5 \times 10^6$  cells/mL) were treated with selective compounds ( $1/3$  of the IC<sub>50</sub> concentration) for 16 hours. After washing in PBS,  $1 \times 10^6$  cells were resuspended in 100 µL of annexin binding buffer. FITC-Annexin V and propidium iodide were added and then incubated for 15 minutes at room temperature in the dark. After the incubation period, 400 µL of annexin-binding buffer was added then kept in an ice bath for 5 minutes. Cells were centrifuged and fixed in 1% formalin. Cells were resuspended in 1% FBS and 0.5% in BSA after centrifugation and then these were analyzed by flow cytometry (BD FACSAria III).

### Acknowledgements

VKS acknowledges CSIR, New Delhi, India for the financial support (Project No. 01/2733/13/EMR-II). One of the authors, R. Kadu acknowledges UGC, New Delhi, India for the financial support in the form of fellowship. We also thank the Department of Science and Technology (DST), New Delhi for the PURSE project under which the single crystal X-ray diffractometer was acquired in the Faculty of Science. We would like to thank Dr. Sanjio Zade for his help in computational study.

**Supporting Information Available:** Synthesis, Characterization, Crystallographic (CIF) (CCDC No. 986523 for **6**, 986524 for **5**, 986525 for **7.DMSO**, 986526 for **7.2CH<sub>2</sub>Cl<sub>2</sub>** and 1426720 for **8.CHCl<sub>3</sub>.8H<sub>2</sub>O**), Computational and TG-DTA data.

## References

- (a) C. J. Jones, *Chem. Soc. Rev.*, 1998, 27, 289. (b) G. F. Swiegers and T. J. Malefetse, *Chem. Rev.*, 2000, 100, 3483. (c) S. Leininger, B. Olenyuk and P. Stang, *Chem. Rev.*, 2000, 100, 853. (d) B. J. Holliday and C. A. Mirkin, *Angew. Chem., Int. Ed.*, 2001, 40, 2022. (e) M. Eddaoudi, D. B. Moler, H. Li, B. Chen, T. M. Reineke, M. O.-Keeffe and O. M. Yaghi, *Acc. Chem. Res.*, 2001, 34, 319. (f) O. K. Farha, J. T. Hupp, *Acc. Chem. Res.*, 2010, 43, 1166.
- (a) H. Ito, T. Kusukawa and M. Fujita, *Chem. Lett.*, 2000, 29, 598. (b) R. Cacciapaglia, S. D. Stefano and L. Mandolini, *Acc. Chem. Res.*, 2004, 37, 113. (c) S. P. Argent, T. R.-Johannessen, J. C. Jeffery, L. P. Harding and M. D. Ward. *Chem. Commun.* 2005, 4647. (d) M. D. Pluth, R. G. Bergman and K. N. Raymond, *Acc. Chem. Res.*, 2009, 42, 1650. (e) A. Corma, H. García and F. X. L-Xamena, *Chem. Rev.*, 2010, 110, 4606. (f) O. D. Fox, J. Cookson, E. J. S. Wilkinson, M. G. B. Drew, E. J. MacLean, S. J. Teat and P. D. Beer, *J. Am. Chem. Soc.*, 2006, 128, 6990. (g) D. Fielder, R. G. Bergman and K. N. Raymond, *Angew. Chem., Int. Ed.*, 2004, 43, 6748. (h) M. Yoshizawa, Y. Takeyama, T. Okano and M. Fujita, *J. Am. Chem. Soc.*, 2003, 125, 3243. (i) M. L. Merlau, M. P. Meija, S. T. Nguyen and J. T. Hupp, *Angew. Chem., Int. Ed.*, 2001, 40, 4239. (j) Z. R. Bell, L. P. Harding and M. D. Ward, *Chem. Commun.*, 2003, 2432.
- (a) M. Fujita, *Chem. Soc. Rev.*, 1998, 27, 417. (b) M. F. Hawthorne and Z. Zheng, *Acc. Chem. Res.*, 1997, 30, 267. (c) P. D. Beer and P. A. Gale, *Angew. Chem., Int. Ed.*, 2001, 40, 486. (d) B. Chen, S. Xiang and G. Qian, *Acc. Chem. Res.*, 2010, 43, 1115. (e) P. R. A. Webber, M. G. B. Drew, R. Hibbert and P. D. Beer, *Dalton Trans.*, 2004, 1127. (f) W. W. H. Wong, J. Cookson, E. A. L. Evans, E. J. L. McInnes, J. Wolowska, J. P. Maher, P. Bishop and P. D. Beer, *Chem. Commun.*, 2005, 2214.
- (a) R. Pandey, P. Kumar, A. K. Singh, M. Shahid, P.-z. Li, S. K. Singh, Q. Xu, A. Misra, and D. S. Pandey, *Inorg. Chem.*, 2011, 50, 3189. (b) P. D. Beer, *Acc. Chem.*

- Res.*, 1998, 31, 71. (c) B. E.-Aroussi, L. Guénée, P. Pal and Hamacek, *J. Inorg. Chem.*, 2011, 50, 8588.
5. (a) C. Sanchez, B. Julián, P. Belleville and M. Popall, *J. Mater. Chem.*, 2005, 15, 3559. (b) U. Mueller, M. Schubert, F. Teich, H. Puetter, K. S.-Arndt and J. Pastré, *J. Mater. Chem.*, 2006, 16, 626. (c) V. Finsy, H. Verelst, L. Alaerts, D. D.-Vos, P. A. Jacobs, G. V. Baron and J. F. M. Denayer, *J. Am. Chem. Soc.*, 2008, 130, 7110. (d) L. Duan, Z.-H. Wu, J.-P. Ma, X.-W. Wu and Y.-B. Dong, *Inorg. Chem.*, 2010, 49, 11164.
6. F. B. L. Cougnon and J. K. M. Sanders, *Acc. Chem. Res.*, 2012, 45, 2211.
7. (a) J. Olguín, M. Kalisz, R. Clérac and S. Brooker, *Inorg. Chem.*, 2012, 51, 5058. (b) A. L. Gavrilova and B. Bosnich, *Chem. Rev.*, 2004, 104, 349. (c) J. Klingele, S. Dechert and F. Meyer, *Coord. Chem. Rev.*, 2009, 253, 2698. (d) T. W. Hambley, *Dalton Trans.*, 2007, 4929. (e) C. Orvig and M. J. Abrams, *Chem. Rev.*, 1999, 99, 2201. (f) K. H. Thompson and C. Orvig, *Dalton Trans.*, 2006, 761.
8. P. C. A. Bruijninx and P. J. Sadler, *Curr. Opin. Chem. Biol.*, 2008, 12, 197.
9. (a) Y. W. Jung and S. J. Lippard, *Chem. Rev.*, 2007, 107, 1387. (b) S. K. Singh, S. Joshi, A. R. Singh, J. K. Saxena and D. S. Pandey, *Inorg. Chem.*, 2007, 46, 10869. (c) R. K. Gupta, R. Pandey, G. Sharma, R. Prasad, B. Koch, S. Srikrishna, P.-Z. Li, Q. Xu and D. S. Pandey, *Inorg. Chem.*, 2013, 52, 3687. (d) R. K. Gupta, G. Sharma, R. Pandey, A. Kumar, B. Koch, P.-Z. Li, Q. Xu and D. S. Pandey, *Inorg. Chem.*, 2013, 52, 13984.
10. (a) G. N. Kaluđerović, H. Kommera, E. H.-Hawkins, R. Paschke and S. G.-Ruiz, *Metallomics*, 2010, 2, 419. (b) T. Boulikas, A. Pantos, E. Bellis and P. Christofis, *Cancer Ther.*, 2007, 5, 537. (c) S. van Zutphen and Reedijk, *J. Coord. Chem. Rev.*, 2005, 249, 2845. (d) R. Gust, W. Beck, G. Jaouen and H. Schoenenberger, *Coord. Chem. Rev.*, 2009, 253, 2760. (e) R. Gust, W. Beck, G. Jaouen and H. Schoenenberger, *Coord. Chem. Rev.* 2009, 253, 2742.
11. (a) G. Hogarth, *Mini-Reviews in Medicinal Chemistry*, 2012, 12, 1202. (b) J. C. Joyner, J. Reichfield and J. A. Cowan, *J. Am. Chem. Soc.* 2011, 133, 15613. (c) J. Lv, T. Liu, S. Cai, X. Wang, L. Liu and Y. Wang, *J. Inorg. Biochem.*, 2006, 100, 1888.
12. (a) T. Wang and Z. J. Guo, *Curr. Med. Chem.*, 2006, 13, 525. (b) F. Tisato, C. Marzano, M. Porchia, M. Pellei and C. Santini, *Med. Res. Rev.*, 2010, 30, 708. (c) S. Tardito and L. Marchio, *Curr. Med. Chem.*, 2009, 16, 1325. (d) C. Duncan and A. R.

- White, *Metallomics*, 2012, 4, 127. (e) C. Marzano, M. Pelli, F. Tisato and C. Santini, *Med. Chem.*, 2009, 9, 185.
13. (a) E.M. Driggers, S. P. Hale, J. Lee and N. K. Terrett, *Nat. Rev. Drug Discov.*, 2008, 7, 608. (b) J. Mallinson and I. Collins, *Future Med. Chem.*, 2012, 4, 1409. (c) Mann A. Conformational restriction and/or steric hindrance in medicinal chemistry. In: *The Practice Of Medicinal Chemistry*, Wermuth CG (Ed.). Academic Press, London, UK 2008.
14. R. Kieltyka, P. Englebienne, J. Fakhoury, C. Autexier, N. Moitessier, and H. F. Sleiman, *J. Am. Chem. Soc.*, 2008, 130, 10040.
15. R. Kadu, H. Roy and V. K. Singh, *Appl. Organomet. Chem.*, 2015 (Accepted).
16. (a) A. Alama, B. Tasso, F. Novelli and F. Sparatore, *Drug Discovery Today*, 2009, 14, 500. (b) S. Jangir, V. Bala, N. Lal, L. Kumar, A. Sarswat, L. Kumar, B. Kushwaha, P. Singh, P. K. Shukla, J. P. Maikhuri, G. Gupta and V. L. Sharma, *Org. Biomol. Chem.*, 2014, 12, 3090. (c) L. Kumar, A. Sarswat, N. Lal, V. L. Sharma, A. Jain, R. Kumar, V. Verma, J. P. Maikhuri, A. Kumar, P. K. Shukla and G. Gupta, *Eur. J. Med. Chem.*, 2010, 45, 817.
17. (a) Y. Suda, A. Arano, Y. Fukui, S. Koshida, M. Wakao, T. Nishimura, S. Kusumoto and M. Sobel, *Bioconjugate Chem.*, 2006, 17, 1125. (b) A. B. Mahon and P. S. Arora, *Chem. Commun.*, 2012, 48, 1416. (c) S. A. Stoffregen, A. K. K. Griffin and N. M. Kostic, *Inorg. Chem.*, 2005, 44, 8899. (d) S. J. Dougan, A. Habtemariam, S. E. McHale, S. Parsons and P. J. Sadler, *Proc. Natl. Acad. Sci. U.S.A.*, 2008, 105, 11628. (e) B. P. Espósito and R. Najjar, *Coord. Chem. Rev.*, 2002, 232, 137.
18. (a) G. A. Bain, D. X. West, J. Krejci, J. Valdes, H. A. Simon and R. A. Toscano, *Polyhedron*, 1997, 16, 855. (b) S. Chavan and R. Sivappa, *Tetrahedron Lett.*, 2004, 45, 3941. (c) K. Parang, E. E. Knaus, L. I. Wiebe, S. Sardari, M. Daneshtalab and F. Csizmadia, *Arch. Pharm.*, 1996, 37, 671. (d) P. Rathelot, N. Azas, H. El-Kashef, F. Delmas, C. Di Giorgio, P. Timon-David, J. Maldonado and P. Vanelle, *Eur. J. Med. Chem.*, 2002, 37, 671. (e) R. P. Pawar, N. M. Andurkar and Y. B. Vibhute, *J. Indian Chem. Soc.*, 1999, 76, 271. (f) A. A. Bekhit, T. Y. Hesham, A. F. Sherif and A. M. Baraka, *Eur. J. Med. Chem.*, 2003, 38, 27. (g) N. Irbas and R. Glu, *Turk. J. Chem.*, 2004, 28, 679. (h) S. Pandey, D. Sriram, G. Nath and E. DeClercq, *Eur. J. Pharm. Sci.*, 1999, 9, 25.
19. (a) R. S. Collinson and D. E. Fenton, *Coord. Chem. Rev.*, 1996, 148, 19. (b) M. Gielen, *Coord. Chem. Rev.*, 1996, 151, 41.

20. (a) R. Sylvain, J. L. Bernier and M. J. Waring, *J. Org. Chem.*, 1996, 61, 2326. (b) B. Santanu and S. M. Subbrangsu, *J. Chem. Soc., Chem. Commun.*, 1995, 2489. (c) D. J. Gravert and J. H. Griffin, *J. Org. Chem.*, 1993, 58, 820.
21. K. Tanaka, T. Ino, T. Sawahata, S. Marui, H. Igaki and H. Yashima, *Mutat. Res.*, 1985, 143, 11.
22. V. K. Singh, R. Kadu and H. Roy, *Eur. J. Med. Chem.*, 2014, 74, 552.
23. R. Kadu, V. K. Singh, S. K. Verma, P. Raghavaiah and M. M. Shaikh *J. Mol. Struct.*, 2013, 1033, 298.
24. A. T. Veetil, T. Šolomek, B. P. Ngoy, N. Pavlíková, D. Heger and P. Klán, *J. Org. Chem.*, 2011, 76, 8232.
25. P. D. Beer, A. R. Cowley, J. C. Jeffery, R. L. Paul and W. W. H. Wong, *Polyhedron*, 2003, 22, 795.
26. A. L. Johnson, M. S. Hill, G. K.-Köhn, K. C. Molloy and A. L. Sudlow, *Inorg. Chem. Commun.*, 2014, 49, 8.
27. (a) N. Yoshida, H. Oshio and T. Ito, *J. Chem. Soc., Perkin Trans. 2*, 1999, 975. (b) A. Arbuse, S. Mandal, S. Maji, M. A. Martínez, X. Fontrodona, D. Utz, F. W. Heinemann, S. Kisslinger, S. Schindler, X. Sala and A. Llobet, *Inorg. Chem.*, 2011, 50, 6878.
28. Y. Pang, S. Cui, B. Li, J. Zhang, Y. Wang and H. Zhang, *Inorg. Chem.*, 2008, 47, 10317.
29. V. F. Plyusnin, A. V. Kolomeets, V. P. Grivin, S. V. Larionov and H. Lemmetyinen, *J. Phys. Chem. A*, 2011, 115, 1763.
30. (a) G. Hogarth, E.-J. C.-R. C. R. R.-Brent, S. E. Kabir, I. Richards, J. D. E. T. W.-Ely and Q. Zhang, *Inorg. Chim. Acta*, 2009, 362, 2020. (b) S. K.; Verma and V. K. Singh, *RSC Adv.*, 2015, 5, 53036.
31. (a) D. Coucouvanis, *Prog. Inorg. Chem.*, 1979, 26, 301. (b) G. Rajput, V. Singh, S. K. Singh, L. B. Prasad, M. G. B. Drew and N. Singh, *Eur. J. Inorg. Chem.* 2012, 3885.
32. (a) H. P. S. Chauhan and A. Bakshi, *J Therm. Anal. Calorim.*, 2011, 105, 937. (b) A. Singhal, D. P. Dutta, A. K. Tyagi, M. M. Shaikh, P. Mathur and I. Lieberwirth, *J. Organomet. Chem.*, 2007, 692, 5285.
33. 'POWDERX' – A program for indexing and refinement of X-ray data written by Dr. V. K. Wadhavan, Bhabha Atomic research Center, private communication.
34. R. K. Gupta, R. Pandey, R. Singh, N. Srivastava, B. Maiti, S. Saha, P. Li, Q. Xu and D. S. Pandey, *Inorg. Chem.*, 2012, 51, 8916.

35. A. Kochem, H. Kansa, B. Baptiste, H. Arora, C. Philouze, O. Jarjayes, H. Vezin, D. Luneau, M. Orio and F. Thomas, *Inorg. Chem.*, 2012, 51, 10557.
36. N. Yoshida, N. Ito and K. Ichikawa, *J. Chem. Soc., Perkin Trans. 2*, 1997, 2387.
37. J. Manosroi, P. Dhumtanom and A. Manosroi, *Cancer Lett.*, 2006, 235, 114.
38. (a) L. Piazzzi, A. Cavalli, F. Belluti, A. Bisi, S. Gobbi, S. Rizzo, M. Bartolini, V. Andrisano, M. Recanatini and A. Rampa, *J. Med. Chem.*, 2007, 50, 4250. (b) I. P. Ferreira, G. M. de Lima, E. B. Paniago, W. R. Rocha, J. A. Takahashi, C. B. Pinheiro and J. D. Ardisson, *Eur. J. Med. Chem.*, 2012, 58, 493. (c) M. A. Soares, J. A. Lessa, I. C. Mendes, J. G. Da Silva, R. G. dos Santos, L. B. Salum, H. Daghestani, A. D. Andricopulo, B. W. Day, A. Vogt, J. L. Pesquero, W. R. Rocha and H. Beraldo, *Bioorg. Med. Chem.*, 2012, 20, 3396.
39. (a) W. Jiang, Y. Fu, F. Yang, Y. Yang, T. Liu, W. Zheng, L. Zeng and T. Chen, *ACS Appl. Mater. Interfaces*, 2014, 6, 13738. (b) G. Kim, W. Kim, K. Kim and J. Lee, *Appl. Phys. Lett.*, 2010, 96, 021502.
40. (a) D. Wlodkowic, S. Faley, M. Zagnoni, J. P. Wikswo and J. M. Cooper, *Anal. Chem.*, 2009, 81, 5517. (b) D. Wlodkowic, J. Z. Skommer and Darzynkiewicz, *Cytometry, Part A*, 2008, 73, 496. (c) D. Hanahan and R. A. Weinberg, *Cell*, 2000, 100, 57. (d) D. Wlodkowic, J. Skommer, S. Faley, Z. Darzynkiewicz and J. M. Cooper, *Exp. Cell Res.*, 2009, 315, 1706.
41. (a) D. Oltmanns, S. Z.-Kolbe, A. Mueller, U. B.-Wuest, M. Schaefer, M. Eder, U. Haberkorn and M. Eisenhut, *Bioconjugate Chem.*, 2011, 22, 2611.
42. (a) "CrysAlispro" program (Version 1.171.37.33 Agilent Technologies, 2014). (b) Bruker SMART V5.630 and SAINT-PLUS V6.45, Bruker-Nonius Analytical X-ray Systems Inc.: Madison, Wisconsin, USA, 2003. (c) SADABS 1997 Empirical absorption correction program, Bruker AXS Inc., Madison, Wisconsin, USA.
43. G. M. Sheldrick, SHELXL-97: program for crystal structure refinement, University of Göttingen, Göttingen, Germany, 1997.
44. Olex2 (version 1.2.5) program package: O. V. Dolomanov, L. J. Bourhis, R. J. Gildea, J. A. K. Howard and H. Puschmann, OLEX2: A complete structure solution, refinement and analysis program. *J. Appl. Cryst.*, 2009, 42, 339.